

## Electronic and transport properties of rectangular graphene macromolecules and zigzag carbon nanotubes of finite length

A. V. Nikolaev,<sup>1,2</sup> A. V. Bibikov,<sup>1</sup> A. V. Avdeenkov,<sup>1</sup> I. V. Bodrenko,<sup>1</sup> and E. V. Tkalya<sup>1</sup>

<sup>1</sup>*Institute of Nuclear Physics, Moscow State University, Vorob'evy Gory, 119992 Moscow, Russia*

<sup>2</sup>*Institute of Physical Chemistry of RAS, Leninskii pr. 31, 119991 Moscow, Russia*

(Received 10 November 2008; revised manuscript received 9 December 2008; published 21 January 2009)

We study one-dimensional (1D) carbon ribbons with the armchair edges and the zigzag carbon nanotubes and their counterparts with finite length [zero dimension (0D)] in the framework of the Hückel model. Using boundary conditions we derive energy spectra for 1D carbon ribbons. At the Fermi level we construct the explicit solutions and prove the rule of metallicity. We show that the dispersion law (electron band energy) of a 1D metallic ribbon or a 1D metallic carbon nanotube has a universal *sinelike* dependence at the Fermi energy which is independent of its width. We find that in case of metallic graphene ribbons of finite length (rectangular graphene macromolecules) or nanotubes of finite length the discrete energy spectrum in the vicinity of  $\varepsilon=0$  (Fermi energy) can be obtained exactly by selecting levels from the same dispersion law. In case of a semiconducting graphene macromolecule or a semiconducting nanotube of finite length, the positions of energy levels around the energy gap can be approximated with a good accuracy. The electron spectrum of 0D carbon structures often includes additional states at energy  $\varepsilon=0$ , which are localized on zigzag edges and do not contribute to the volume conductivity.

DOI: 10.1103/PhysRevB.79.045418

PACS number(s): 73.22.-f, 73.20.-r, 73.23.-b

Carbon-based materials of nanosize in the form of carbon nanotubes (CNTs) are known for several years and attracted much attention of researchers because of their unusual electronic properties.<sup>1-3</sup> Recently, progress in the fabrication of other graphene-based lower-dimensional structures has been reported.<sup>4,5</sup> This put forward such nanoscaled quantum objects as one-dimensional (1D) carbon ribbons (CRs) (Refs. 6-10) and zero-dimensional (0D) carbon dots.<sup>5,8,11</sup>

Graphene—a two-dimensional (2D) carbon material—was first isolated by micromechanical cleavage of graphite.<sup>12</sup> Its planar hexagonal lattice is formed by  $sp^2$  hybridized carbon bonds. Although graphene is the building block of many carbon allotropes, its electronic structure differs from other carbon materials. At present, the electronic structure and transport properties of 1D CNTs are well understood theoretically<sup>13</sup> and the focus is shifted toward CRs and 0D carbon objects.<sup>14</sup> In particular, it is known that in the framework of the tight-binding model both CRs and CNTs (1D nanomaterials) can be either semiconducting with a size-dependent gap or metallic.<sup>6,7,15,16</sup> It should be also noted that recent density-functional theory (DFT) calculations within local-density approximation (LDA) (DFT-LDA) predict that all armchair CRs are semiconducting, with one group showing small energy gaps.<sup>16-18</sup> We will not discuss this issue here and limit our consideration by the tight-binding (1D) and Hückel models (0D). The rule of metallicity for armchair CRs (the number of carbon rings is equal to  $2+3N$ ) was formulated under assumption that the ribbons are wide enough, so that one can use solutions obtained for graphene semiplane.<sup>15,19</sup> Solving the problem perturbatively [Eq. (1) with  $\delta=0$ ]<sup>16</sup> and numerically, Son *et al.*<sup>16</sup> showed that the rule holds for CRs of any width. Below, in our approach we will obtain the rule of metallicity and the corresponding electronic solutions at  $\varepsilon_F$  in explicit form. Furthermore, we show that for the chosen class of 1D metallic carbon systems the dispersion law of the electronic band crossing the Fermi

level can be obtained analytically [see Eq. (8) below]. Later we generalize the law for 0D systems [Eqs. (14a) and (14b) below]. Throughout the paper we employ the Hückel model and limit ourselves to the class of zigzag CNTs and CRs with the armchair profile. These two materials are closely related with each other. Indeed, by rolling up a 1D armchair CR one obtains a 1D zigzag CNT. (The terms armchair for the ribbon and zigzag for the nanotube are confusing here since they apply to different characteristics: armchair to the edges of the ribbon, while zigzag to the circumference of the nanotube.) On the other hand, all CRs of finite length can be considered as rectangular graphene macromolecules (RGMs) whose electronic properties are important for designing various nanomaterials.

The energy spectrum of nanographite materials (1D CRs, 1D CNTs, 0D RGM, and 0D CNTs) can be obtained from the dispersion relation of graphene,<sup>20</sup>

$$\varepsilon_{\pm} = \varepsilon_F \pm \beta |e^{-iak_y\sqrt{3}/2} + 2 \cos ak_x/2|, \quad (1)$$

where  $a = \sqrt{3}d_{CC}$  and  $d_{CC}$  is the carbon-carbon distance. Here the  $2\pi$  factor is incorporated in  $k$  and  $-\beta$  stands for the Hückel transfer integral (or  $-t$  in the tight-binding model), so that  $\beta > 0$ . At the  $K$  point of the Brillouin zone of graphene two bands intersect,

$$ak_x^K = \pm \frac{4\pi}{3}, \quad (2a)$$

$$ak_y^K = 0. \quad (2b)$$

We start with studying energy spectrum of 1D CRs. The problem is how to reduce the problem to that for graphene. In the unit cell of a zigzag carbon ribbon there are four carbon atoms with two nearest neighbors, while in graphene each carbon atom has three nearest neighbors (Fig. 1). Therefore, if we consider the ribbon as a part of the graphene 2D

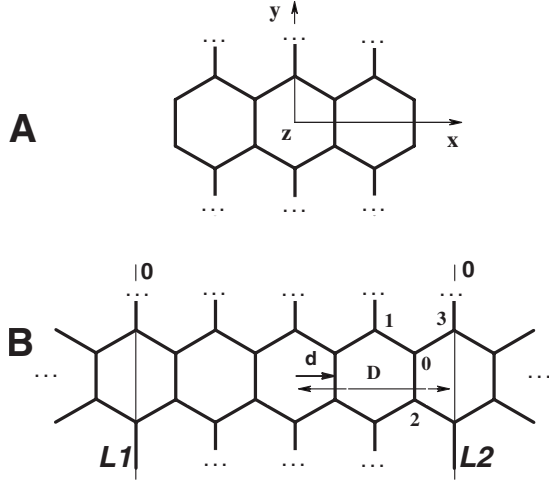


FIG. 1. Boundary conditions for (a) a 1D carbon ribbon and (b) the same ribbon placed in the graphene sheet. Carbon sites on lines  $L_1$  and  $L_2$  have zero coefficients of expansion.

plane [Fig. 1(b)], the equations for the edge atoms of the ribbon are modified. For example, for site 0 in Fig. 1(b) we have

$$\frac{\varepsilon}{\beta}c_0 = -(c_1 + c_2 + c_3), \quad (3)$$

where  $c_i$ ,  $i=0,1,2,3$  are coefficients of the expansion of graphene wave function  $\psi_g$ . However, if we set  $c_3=0$ , then Eq. (3) will be identical to that for the ribbon. Thus, we can select the solutions for the CR out of the graphene solutions by requiring  $c_j=0$  for all carbon sites  $j$  on lines  $L_1$  and  $L_2$  and by repeating the resulting pattern in the  $x$  direction. The lines with  $\psi_r=0$  completely separate neighboring nanoribbons from each other since there is no interaction between them.

We arrive at the following conditions of quantization:

$$\cos(Dk'_x) = 0, \quad (4a)$$

$$\sin(Dk'_x) = 0. \quad (4b)$$

Here  $D=md$  ( $m$  is an integer) and  $d=\sqrt{3}d_{CC}/2$ . [Both distances are shown in Fig. 1(b).] The number of carbon rings in the  $x$  direction is  $\mathcal{N}=m-1$ . It is clear that the CR will be metallic if line  $(k'_x, k'_y)$  in  $k$  space goes through the  $K$  point [Eqs. (2a) and (2b)]. Solving Eqs. (4a) and (4b) leads to

$$ak'_x = 2\pi\frac{n}{m}, \quad (5)$$

where  $n$  is an integer number. Condition (5) coincides with Eqs. (2a) and (2b) only if

$$m = 3m', \quad (6a)$$

$$n = 2m'. \quad (6b)$$

This immediately gives

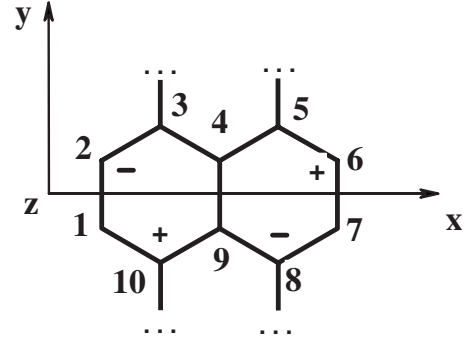


FIG. 2. Unit cell of 1D metallic carbon ribbon. Plus signs (sites 6 and 10) and minus signs (sites 2 and 8) refer to eigenvector  $V_1$  at  $\varepsilon_F=0$ .

$$\mathcal{N} = 3m' - 1. \quad (7)$$

Equation (7) determines which CR is metallic.<sup>15,16</sup> We get  $\mathcal{N}=2, 5, 8, \dots$ . Substituting  $(k'_x=k_x^K, k'_y=k)$  in Eq. (1) leads to the dispersion relations for two bands which cross at the Fermi energy

$$\varepsilon_{\pm} = \varepsilon_F \pm 2\beta \sin\frac{Xk}{4}, \quad (8)$$

where  $X=3d_{CC}$  ( $X$  is the modulus of the basis vector in the  $y$  direction). The corresponding density of states (DOS) *per unit cell* (for both spins projections) in the neighborhood of  $\varepsilon_F=0$  is given by

$$\rho(\varepsilon) = \frac{2}{\pi} \frac{1}{\sqrt{1 - (\varepsilon/2\beta)^2}} \frac{1}{\beta}. \quad (9)$$

Equation (9) coincides with that for metallic CNTs.<sup>13</sup>

It is instructive to study the two electronic states at the Fermi energy when  $k_F=0$ . We start by considering the simplest possible case:  $\mathcal{N}=2$  (Fig. 2). Then the following explicit eigenvectors can be found:

$$V_1 = \frac{1}{2}\{0, -1, 0, 0, 0, 1, 0, -1, 0, 1\}, \quad (10a)$$

$$V_2 = \frac{1}{2}\{-1, 0, 1, 0, -1, 0, 1, 0, 0, 0\}. \quad (10b)$$

$V_1$  is visualized in Fig. 2 by putting plus and minus signs at corresponding carbon sites.  $V_2$  is obtained from  $V_1$  through the mirror reflection at the  $xz$  plane, which follows from the symmetry of the electronic system. In this way one can construct two eigenvalues for any metallic CR. As an example in Fig. 3 we schematically draw one eigenvector for a CR with the eight-ring unit cell. Notice that all three blocks have the structure of  $V_1$  (Fig. 2). The blocks are connected via chains of carbon sites, lines  $L_1$  and  $L_2$ , where  $c_j=0$ . As before, the second eigenvector is obtained from the first through the  $xz$ -mirror reflection. Thus, we can build two eigenvectors only if the number of blocks is  $\mathcal{N}=2+3n$ , which also gives rule (7).

From Eq. (1) one can derive the expression for energy gap  $E_g$  if  $\mathcal{N} \neq 3m' - 1$ . There are two cases: (1)  $\mathcal{N}=3m'$  and  $m$

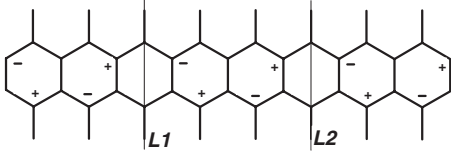


FIG. 3. Unit cell of 1D metallic carbon ribbon containing eight carbon rings. Plus and minus signs schematically indicate one of two eigenvectors at  $\varepsilon_F=0$ .

$=3m'+1$  and (2)  $\mathcal{N}=3m'-2$  and  $m=3m'-1$ . In both cases the energy gap is given by

$$E_g = 2\beta \left| 1 - \cos \frac{\delta\phi}{2} - \sqrt{3} \sin \frac{\delta\phi}{2} \right|, \quad (11a)$$

The value of  $\delta\phi$  depends on which branch, Eq. (4a) or (4b), is considered. (It is a measure of deviation from the  $K$  point [Eqs. (2a) and (2b) in the zone-folding model].) For cosine-like branches [Eq. (4a)] we get  $n=2m'$  [Eq. (6b)] and

$$\delta\phi_{\cos} = \mp \frac{\pi}{3(\mathcal{N}+1)}. \quad (11b)$$

Here the first choice of  $\mathcal{N}$  corresponds to minus sign, while the second choice of  $\mathcal{N}$  corresponds to plus sign. For sine-like branches [Eq. (4a)] we get

$$\delta\phi_{\sin} = 4\phi_{\cos}, \quad n = 2m', \quad (11c)$$

$$\delta\phi_{\sin} = 2\phi_{\cos}, \quad n = 2m' \pm 1. \quad (11d)$$

By comparing Eq. (11b) with Eqs. (11c) and (11d) we conclude that the gap is due to cosinelike branches [Eq. (11b)]. If  $\delta\phi_{\cos} \ll 1$ , which is often the case,

$$E_g = \beta \frac{4\pi}{\sqrt{3}} \frac{1}{\mathcal{N}+1}. \quad (12)$$

Thus,  $E_g \sim 1/\mathcal{N}$  as it was the case for CNTs.<sup>13</sup>

The rule for the metallicity of armchair CRs [Eq. (7)] is very different from the rule for the corresponding zigzag CNTs characterized by the pair of indices  $[\mathcal{N}, 0]$  as follows:

$$\mathcal{N} = 3m'. \quad (13)$$

It is clear that the rules do not overlap, meaning that if one rolls up a nanotube from a metallic ribbon, then the resultant nanotube will not be metallic and vice versa. This conclusion deserves a more detailed explanation. We notice that the metallicity rule for CNTs [Eq. (13)] is obtained from the cyclic condition in the  $x$  direction which allows for sine-like and cosine-like dependencies, while in case of ribbon only sine-like functions are allowed. (One can prove that Eq. (4a) does not include the  $K$  point [Eq. (2a)].) The sine dependence in the  $x$  direction implies opposite signs for coefficients  $c_j$  belonging to edge sites  $j$  on opposite sides of CR. By rolling up a nanotube the carbon sites on opposite edges of ribbon should coincide, which in turn destroys the odd solutions. The even solutions satisfying the cyclic condition survive the rolling up procedure but none of them has energy at  $\varepsilon_F=0$ .

We now turn to 0D objects—carbon macromolecules and

TABLE I. Length dependence of the energy spectrum of metallic RGMs ( $\mathcal{N}=2,5,\dots$ ) and CNTs ( $\mathcal{N}=3,6,\dots$ ).

| HOMO- $i$ | Length (in $d_{CC}$ ) |          |          |
|-----------|-----------------------|----------|----------|
|           | 299                   | 149      | 29       |
| 1         | -0.00783              | -0.01563 | -0.07661 |
| 2         | -0.02350              | -0.04689 | -0.22937 |
| 3         | -0.03917              | -0.07813 | -0.38078 |
| 4         | -0.05483              | -0.10935 | -0.52996 |
| 5         | -0.07049              | -0.14055 | -0.67603 |
| 6         | -0.08615              | -0.17172 | -0.81814 |
| 7         | -0.10180              | -0.20284 | -0.95544 |

nanotubes of finite length. Unlike 1D electron systems characterized by electron energy band structure, they have discrete energy spectra. However, these spectra are closely related with electron bands which we have already considered. In particular, energy levels of RGMs and CNTs near the Fermi energy are described by the following expression:

$$\varepsilon_{\pm}(n) = \pm 2\beta \sin \frac{Xk(n)}{4}, \quad (14a)$$

where

$$k(n) = \delta k \left( n + \frac{1}{2} \right), \quad (14b)$$

$n=0,1,2,\dots$ ,  $\delta k = \pi/L$ , and  $L=L_0+7d_{CC}/4$ . Here  $L_0$  is the length of nanotube or ribbon (maximal distance between carbon atoms in the  $y$  direction, which has the armchair profile). We want to stress that Eqs. (14a) and (14b) are *exact* (see the Appendix). The electron spectrum given by Eq. (14a) is independent of width which is consistent with the situation observed for 1D objects. It is also worth noting that the spectrum of 0D carbon objects consists of many discrete levels and instead of Fermi level we should speak of highest occupied molecular orbital (HOMO) and lowest unoccupied molecular orbital (LUMO). This implies that formally we cannot speak of metallicity and semiconductivity. However, in Tables I–III we retain these terms in a loose sense, because from one side, it shows relations with corresponding 1D objects and from the other side the existence or nonexistence of a large energy gap at the HOMO-LUMO region remains one of the important characteristics of these systems.

It is clear that Eqs. (14a) and (14b) can be considered as a discretization of Eq. (8). Following this route we can derive an approximate expression for nonmetallic RGMs and CNTs. We recall that for 1D systems there are various bands, which we have discussed already while calculating  $E_g$ . In general their energy is

$$\frac{\varepsilon_{\pm}}{\beta} = \pm \left| e^{-i(X/2)k} - \cos \frac{\delta\phi}{2} - \sqrt{3} \sin \frac{\delta\phi}{2} \right|, \quad (15)$$

where  $\delta\phi = \delta\phi_{\sin}$  or  $\delta\phi_{\cos}$ . The highest occupied band for RGMs is given by  $\delta\phi_{\cos}$  [Eq. (11b)]. Starting with Eq. (15) and taking inspiration from the relation between Eqs. (8) and

TABLE II. Length dependence of the energy spectrum of semiconducting RGM;  $\mathcal{N}=10$  ( $L_0=3.5d_{CC}$ ,  $\delta=0.9$ ). ‘‘Exact’’ refers to the straightforward Hückel calculations and ‘‘approx.’’ to the values of Eqs. (16a) and (16b).

| HOMO- $i$ | $299d_{CC}$ |          | $214d_{CC}$ |          |
|-----------|-------------|----------|-------------|----------|
|           | Exact       | Approx.  | Exact       | Approx.  |
| 1         | -0.08271    | -0.08258 | -0.08371    | -0.08356 |
| 2         | -0.08689    | -0.08691 | -0.09069    | -0.09100 |
| 3         | -0.09349    | -0.09388 | -0.10143    | -0.10250 |
| 4         | -0.10210    | -0.10294 | -0.11501    | -0.11687 |
| 5         | -0.11230    | -0.11360 | -0.13064    | -0.13318 |
| 6         | -0.12374    | -0.12544 | -0.14771    | -0.15079 |
| 7         | -0.13611    | -0.13816 | -0.16580    | -0.16928 |

(14a) we obtain the discretized version for  $\varepsilon_{\pm}(n)$  of semiconducting RGMs or CNTs of finite length,

$$\frac{\varepsilon_{\pm}(n)}{\beta} = \pm \left| e^{-i(X/2)k'(n)} - \cos \frac{\delta\phi}{2} - \sqrt{3} \sin \frac{\delta\phi}{2} \right|, \quad (16a)$$

$$k'(n) = \delta k(n + \delta). \quad (16b)$$

Here  $n=0, 1, 2, \dots$  is integer,  $\delta k = \pi/L$ , and  $L=L_0 + \delta L$ . In fact, in Eq. (16b)  $\delta L \sim d_{CC}$  and  $\delta \sim 1$  are phenomenological parameters which should be found by fitting a data set of  $\varepsilon(n)$ . The set can be taken from a Hückel calculation of RGMs and CNTs or even from a more advanced calculation (such as density functional, for example). In Tables II and III we compare energy spectra given by Eqs. (16a) and (16b) (approx.) with straightforward Hückel calculations (exact).  $\delta\phi$  in Eq. (16a) is  $\phi_{\cos}$  [Eq. (11b)] for graphene molecules and

$$\delta\phi = \pm \frac{2\pi}{3\mathcal{N}} \quad (17)$$

in case of semiconducting nanotubes with width  $\mathcal{N} = 3m' \pm 1$ . The accuracy of Eqs. (16a) and (16b) is on the

TABLE III. Length dependence of the energy spectrum of semiconducting CNT [10, 0] ( $\mathcal{N}=10$ ,  $L_0=3.75d_{CC}$ , and  $\delta=0.9$ ). ‘‘Exact’’ refers to the straightforward Hückel calculations and ‘‘approx.’’ to the values of Eqs. (16a) and (16b).

| HOMO- $i$ | $299d_{CC}$ |          | $214d_{CC}$ |          |
|-----------|-------------|----------|-------------|----------|
|           | Exact       | Approx.  | Exact       | Approx.  |
| 1         | -0.17634    | -0.17623 | -0.17691    | -0.17673 |
| 2         | -0.17864    | -0.17847 | -0.18088    | -0.18067 |
| 3         | -0.18241    | -0.18226 | -0.18733    | -0.18723 |
| 4         | -0.18756    | -0.18750 | -0.19602    | -0.19615 |
| 5         | -0.19400    | -0.19406 | -0.20671    | -0.20712 |
| 6         | -0.20161    | -0.20182 | -0.21910    | -0.21982 |
| 7         | -0.21027    | -0.21065 | -0.23296    | -0.23398 |

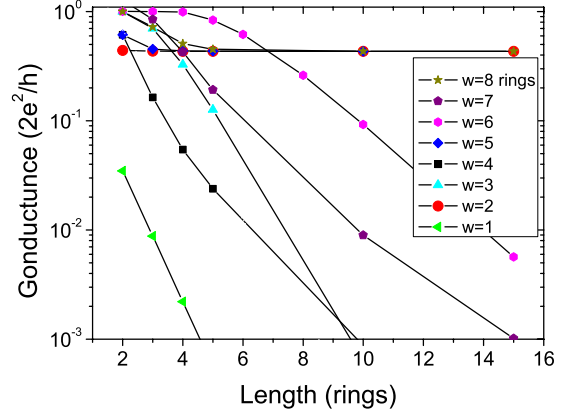


FIG. 4. (Color online) Conductance versus RGM length at  $\varepsilon_F = 0$ .

order of  $10^{-3}\beta$  for ten top occupied molecular orbitals (or HOMO- $i$ ,  $i=1-10$ ) (Tables II and III).

Finally, we remark on the doubly degenerate HOMO level at  $\varepsilon \approx 0$ .<sup>6,15,19</sup> The nature of the states, which are always present in the electronic spectrum of carbon ribbons and nanotubes of finite length, is an object of intense research.<sup>6,15,19,21-25</sup> These states are edge ones because as follows from Eqs. (14a) and (14b)  $\varepsilon_{\text{HOMO}-1} = -2\beta \sin(X\delta k/8) \neq 0$ . The coefficients of the wave function expansion,  $c_j$ , in this case quickly fall to zero as we move away from the edges, and the states do not contribute to the conductivity in the  $y$  direction (Fig. 1). To demonstrate it we have calculated the conductance of RGMs using the Landauer formula.<sup>26</sup> For a qualitative treatment, we define the self-energy within the broadband approximation,<sup>27</sup> considering it as an energy-independent imaginary constant  $\Sigma = i\Delta$  ( $\Delta = 1$  eV). In Fig. 4 we plot conductance as a function of length at  $\varepsilon_F = 0$  for RGMs of various width. Our results show that metallic RGMs ( $n=2, 5, 8$ ) have a weak dependence on length. Their conductances coincide starting with a rather short length of two to six rings. For other nonmetallic RGMs the calculations demonstrate an exponential decrease in conductance with length. It is also worth noting that the conductance of metallic RGMs is always the same and equal to the conductance of the metallic RGM with the minimal width of two rings. (A detailed qualitative and quantitative analysis will be given elsewhere.)

In conclusion, we have studied the electronic spectrum of the 1D armchair CRs and zigzag CNTs and their 0D counterparts of finite length in the Hückel model. We have found the solutions by reducing the problem to that for graphene with appropriate selection rules imposed by boundary conditions. In the vicinity of the HOMO-LUMO energy region ( $\varepsilon \sim 0$ ) we have found the exact expression for energy spectrum of metallic nanosystems [Eqs. (14a) and (14b)] and approximate energy spectrum in case of semiconducting materials [Eqs. (16a) and (16b)]. Finally, we have calculated the conductance of some RGMs and investigated the role of edge states.

The authors would like to thank D. S. Kosov for helpful discussions.



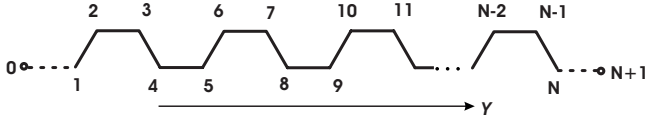


FIG. 5. Effective 1D chain of  $N$  carbon atoms [ $i=1, 2, \dots, N$ ] within the  $l$  ribbon. Also shown are two auxiliary carbon atoms [ $i=0$  and  $i=(N+1)$ ]; see text for details.

## APPENDIX

Here we discuss the derivation of Eqs. (14a) and (14b). For a 1D armchair CR or 1D zigzag CNT each of the discrete values of  $k'_x$  determines an electronic band. The metallic band is given by Eq. (2a) and obtained for Eq. (4b) condition of quantization. This condition implies the  $\sin[(2\pi/3)(x/d)]$  modulation in the  $x$  direction with zero coefficients at  $x/d=3l$ , where  $l=0, 1, 2, \dots$  (Distances and axes are shown in Fig. 1.) Each index  $l$  defines a carbon ribbon in the  $y$  direction with nonzero coefficients at  $x_1/d=1+3l$  and  $x_2/d=2+3l$ . The lines with zero coefficients imply that each ribbon can be considered as independent. In fact, they are equivalent due to the modulation condition [Eq. (4b)]. We can use this property and work only with one ribbon shown in Fig. 5 and later reconstruct the solution for the whole system.

Now we consider one ribbon in the  $y$  direction which is equivalent to a 1D chain of carbon atoms ( $i=1, 2, \dots, N$ ). Considering a solution with the coefficients  $c_j$  of the wave function expansion, we obtain for them the following relations:

$$\frac{\epsilon}{\beta}c_j = -(c_{j-1} + c_{j+1}), \quad (\text{A1})$$

where  $j=2, 3, \dots, (N-1)$ . The problem arises due to the two boundary atoms:  $j=1$  and  $j=N$ . To solve this task we will use the trick which we have already applied to 1D ribbon with Eq. (3). That is, we introduce two auxiliary carbon atoms  $j_{b1}=0$  and  $j_{b2}=(N+1)$  and consider an infinite 1D carbon chain beyond them. Notice that for the following the real shape of the 1D chain is immaterial. It can be equally thought of as a 1D linear chain of carbon atoms. For an infinite chain the general solution is  $c_j \sim \exp(-i\phi'j)$ , where  $\phi' = d_{CC}k'_y$  and  $k'_y$  is an effective wave number. Then the coefficients at  $j_b$  should be zero, i.e.,  $c_0 = c_{N+1} = 0$ . This gives a condition of quantization,

$$\sin(L_y k'_y) = 0, \quad (\text{A2})$$

where  $L_y = (N+1)d_{CC}$ . From Eq. (A2) we get

$$k'_y = \frac{\pi}{L_y} r = \frac{\pi}{(N+1)d_{CC}} r. \quad (\text{A3})$$

Here positive integer  $r=1, 2, \dots, N$ . The energy of the 1D chain is obtained from Eq. (A1) as follows:

$$\epsilon/\beta = -2 \cos(\phi') = -2 \sin\left(\frac{\pi}{2} - \phi'\right). \quad (\text{A4})$$

The latter relation can be written as

$$\epsilon/\beta = -2 \sin\left[\frac{\pi}{N+1}\left(n + \frac{1}{2}\right)\right], \quad (\text{A5})$$

where

$$2n = N - 2r. \quad (\text{A6})$$

Notice that  $n=N/2-1, (N/2-2), \dots, -N/2$ . ( $N$  is even because  $N=4N_{\text{hex}}$ , where  $N_{\text{hex}}$  is the number of hexagons in the  $y$  direction.) First  $N/2$  electron states are occupied by  $N$   $\pi$  electrons. Taking into account the length of CR or CNT in the  $y$  direction

$$L_0 = \left(\frac{3}{4}N - 1\right)d_{CC}, \quad (\text{A7})$$

Eq. (A5) can be rewritten as

$$\epsilon/\beta = \mp 2 \sin\left[\frac{3d_{CC}}{4} \frac{\pi}{(L_0 + 7d_{CC}/4)} \left(n' + \frac{1}{2}\right)\right], \quad (\text{A8})$$

where the solution with the minus sign refers to the occupied states at the Fermi level: HOMO ( $n'=0$ ) and the HOMO  $-n'$  levels ( $n'=1, 2, \dots, N/2$ ). The solution with the plus sign refers to the unoccupied states: the LUMO ( $n'=0$ ) and the LUMO  $+n'$  levels ( $n'=1, 2, \dots, N/2$ ). Equation (A8) is equivalent to Eqs. (14a) and (14b). Finally, we would like to note that the equation implies a certain size relation of RGM,  $L'_y = L_0 > L_x$ . The latter condition is needed to assure that a set of levels around the Fermi level is associated with a 1D metal band and separated from other  $k'_x$  levels (other 1D bands). If it is not so ( $L'_y = L_0 < L_x$ ) then the levels described by Eq. (A8) do exist but they are not grouped together. They are mixed up with other  $k'_x$  levels.

<sup>1</sup>S. Iijima, *Nature* (London) **354**, 56 (1991).

<sup>2</sup>M. S. Dresselhaus, G. Dresselhaus, and P. C. Eklund, *Science of Fullerenes and Carbon Nanotubes* (Academic, San Diego, 1996).

<sup>3</sup>R. Saito, G. Dresselhaus, and M. S. Dresselhaus, *Physical Properties of Carbon Nanotubes* (Imperial College Press, London, 1998).

<sup>4</sup>K. S. Novoselov, Z. Jiang, Y. Zhang, S. V. Morozov, H. L. Stormer, U. Zeitler, J. C. Maan, G. S. Boebinger, P. Kim, and A.

K. Geim, *Science* **315**, 1379 (2007).

<sup>5</sup>A. Geim and K. Novoselov, *Nature Mater.* **6**, 183 (2007).

<sup>6</sup>K. Nakada, M. Fujita, G. Dresselhaus, and M. S. Dresselhaus, *Phys. Rev. B* **54**, 17954 (1996).

<sup>7</sup>M. Y. Han, B. Özyilmaz, Y. Zhang, and P. Kim, *Phys. Rev. Lett.* **98**, 206805 (2007).

<sup>8</sup>B. Özyilmaz, P. Jarillo-Herrero, D. Efetov, D. A. Abanin, L. S. Levitov, and P. Kim, *Phys. Rev. Lett.* **99**, 166804 (2007).

<sup>9</sup>H. Zheng, Z. F. Wang, T. Luo, Q. W. Shi, and J. Chen, *Phys. Rev.*

- B **75**, 165414 (2007).
- <sup>10</sup>H. Raza and E. C. Kan, *Phys. Rev. B* **77**, 245434 (2008).
- <sup>11</sup>J. S. Bunch, Y. Yaish, M. Brink, K. Bolotin, and P. L. McEuen, *Nano Lett.* **5**, 287 (2005).
- <sup>12</sup>K. S. Novoselov, A. K. Geim, S. V. Morozov, D. Jiang, Y. Zhang, S. V. Dubonos, I. V. Grigorieva, and A. A. Firsov, *Science* **306**, 666 (2004).
- <sup>13</sup>J.-C. Charlier, X. Blase, and S. Roche, *Rev. Mod. Phys.* **79**, 677 (2007).
- <sup>14</sup>L. Malysheva and A. Onipko, *Phys. Rev. Lett.* **100**, 186806 (2008).
- <sup>15</sup>K. Wakabayashi, M. Fujita, H. Ajiki, and M. Sigrist, *Phys. Rev. B* **59**, 8271 (1999).
- <sup>16</sup>Y.-W. Son, M. L. Cohen, and S. G. Louie, *Phys. Rev. Lett.* **97**, 216803 (2006).
- <sup>17</sup>V. Barone, O. Hod, and G. E. Scuseria, *Nano Lett.* **6**, 2748 (2006).
- <sup>18</sup>C. T. White, J. Li, D. Gunlycke, and J. W. Mintmire, *Nano Lett.* **7**, 825 (2007).
- <sup>19</sup>M. Fujita, K. Wakabayashi, K. Nakada, and K. Kusakabe, *J. Phys. Soc. Jpn.* **65**, 1920 (1996).
- <sup>20</sup>P. R. Wallace, *Phys. Rev.* **71**, 622 (1947).
- <sup>21</sup>F. Munoz-Rojas, D. Jacob, J. Fernandez-Rossier, and J. J. Palacios, *Phys. Rev. B* **74**, 195417 (2006).
- <sup>22</sup>K. Sasaki, S. Murakami, and R. Saito, *Appl. Phys. Lett.* **88**, 113110 (2006).
- <sup>23</sup>Y.-W. Son, M. L. Cohen, and S. G. Louie, *Nature (London)* **444**, 347 (2006).
- <sup>24</sup>O. Hod, V. Barone, and G. E. Scuseria, *Phys. Rev. B* **77**, 035411 (2008).
- <sup>25</sup>Z. Z. Zhang, K. Chang, and F. M. Peeters, *Phys. Rev. B* **77**, 235411 (2008).
- <sup>26</sup>Y. Imry and R. Landauer, *Rev. Mod. Phys.* **71**, S306 (1999).
- <sup>27</sup>V. Mujica, M. Kemp, and M. A. Ratner, *J. Chem. Phys.* **101**, 6856 (1994).